The Astrophysical Journal, 638:1080–1085, 2006 February 20

PROPERTIES OF PLANETARY CAUSTICS IN GRAVITATIONAL MICROLENSING

Cheongho Han
Department of Physics, Institute for Basic Science Research, Chungbuk National University, Chongju 361-763, South Korea;
cheongho@astroph.chungbuk.ac.kr
Received 2005 August 31; accepted 2005 October 12

ABSTRACT

Although some of the properties of the caustics in planetary microlensing have been known, our understanding of them is mostly from scattered information based on numerical approaches. In this paper, we conduct a comprehensive and analytic analysis of the properties of the planetary caustics, which are one of the two sets of caustics in planetary microlensing, those located away from the central star. Under the perturbative approximation, we derive analytic expressions for the location, size, and shape of the planetary caustic as a function of the star-planet separation and the planet/star mass ratio. Based on these expressions combined with those for the central caustic, which is the other set of caustics and is located close to the central star, we compare the similarities and differences between the planetary and central caustics. We also present the expressions for the size ratio between the two types of caustics and for the condition of the merging of the two types of caustics. These analytic expressions will be useful in understanding the dependence of the planetary lensing behavior on the planet parameters and thus in interpreting the planetary lensing signals.

Subject headings: gravitational lensing — planetary systems — planets and satellites: general

Online material: color figures

1. INTRODUCTION

Microlensing is one of the most powerful methods that can be used to search for extrasolar planets (Mao & Paczyński 1991; Gould & Loeb 1992). Recently, two robust microlensing detections of exoplanets were reported by Bond et al. (2004) and Udalski et al. (2005).

The microlensing signal of a planetary companion to a star is a short-duration perturbation to the smooth standard light curve of the primary-induced lensing event occurring on a background source star. The planetary perturbation occurs when the source star passes close to the caustic. The caustic represents the set of source positions at which the magnification of a point source becomes infinite. Studies of the properties of the caustic are important because the characteristics of the planetary perturbations in the microlensing light curve depend critically on the properties of the caustic. For example, the location of the perturbation on the lensing light curve depends on the location of the caustic. The duration of the perturbation and the probability of detecting the perturbation are proportional to the caustic size. In addition, the pattern of the perturbation is closely related to the caustic shape. Therefore, it is essential to understand the properties of caustics for the interpretation of the planetary lensing signals.

Although some of the properties of the caustics in planetary microlensing have been known, our knowledge of them is mostly from scattered information based on numerical approaches. The problem of the numerical approach is that the dependence of the planetary lensing behavior on the planet parameters of the star-planet separation s (normalized by the Einstein ring radius $\theta_{\rm E}$) and the planet/star mass ratio q is not clear. There have been several attempts to overcome this ambiguity using analytic methods. By treating the planet-induced deviation as a perturbation, Dominik (1999) and An (2005) derived analytic expressions for the locations of the *central* caustic, which is one of the two sets of caustics of the star-planet lens system located close to the primary star. Based on a similar perturbational approach, Asada (2002) provides analytic expressions for the locations of the lensing images. Bozza (2000) derived analytic expressions for the locations of not only the central caustic but also the *planetary* caustics, the other set of caustics, which are located away from the central star. However, there has been no analytic work on the detailed properties of the caustics such as the location, size, and shape, except the very recent work of Chung et al. (2005, hereafter Paper I) on the central caustics.

Following Paper I, we conduct a comprehensive and analytic analysis on the properties of the planetary caustics. Under the perturbational approximation, we derive analytic expressions for the location, size, and shape of the planetary caustics as a function of s and q. Based on these expressions combined with those for the central caustics derived in Paper I, we compare the similarities and differences between the planetary and central caustics. We provide an expression for the size ratio between the two types of caustics. We also derive an expression for the condition of the merging of the two types of caustics. We finally discuss the validity of the perturbational approximation.

2. EMPIRICAL KNOWN PROPERTIES

A planetary lensing is described by the formalism of a binary lens with a very low mass companion. Because of the very small mass ratio, planetary lensing behavior is well described by that of a single lensing of the primary star for most of the event duration. However, a short-duration perturbation can occur when the source star passes the region around the caustics, which are important features of binary lensing.

The caustics of binary lensing form single or multiple closed figures, each of which is composed of concave curves (fold caustics) that meet at cusps. For a planetary case, there exist two sets of disconnected caustics. The central caustic is located close to the host star. The planetary caustic is located away from the host star, and there are one or two sets of disconnected caustics depending on whether the planet lies outside ($s > 1$) or inside ($s < 1$) the Einstein ring. The size of the caustic, which is directly proportional to the planet detection efficiency, is maximized

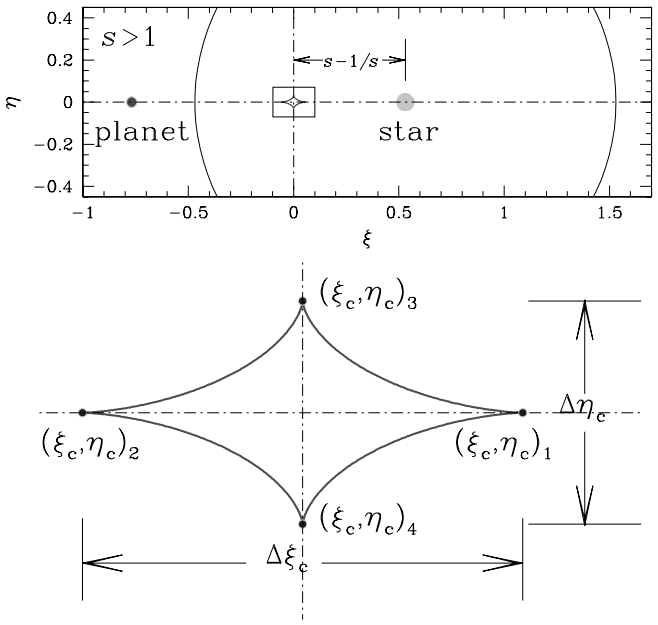

FIG. 1.—Location and shape of the planetary caustic of a planetary system with a star-planet separation greater than the Einstein ring radius ($s > 1$). The top panel shows the location of the star, the planet, and the resulting location of the planetary caustic. The coordinates are centered at the center of the planetary caustic, which is located on the star-planet axis with a separation vector $\boldsymbol{r} = \boldsymbol{s}(1 - 1/s^2)$ from the position of the star, where $\boldsymbol{s}$ is the position vector of the planet from the host star. The circle centered at the position of the star is the Einstein ring. The bottom panel shows a blow up of the region around the caustic enclosed by a box. Also marked are the definitions of the horizontal ($\Delta\xi_c$) and vertical ($\Delta\eta_c$) widths of the caustic and the designations of the individual cusps of the caustic. [*See the electronic edition of the Journal for a color version of this figure*.]

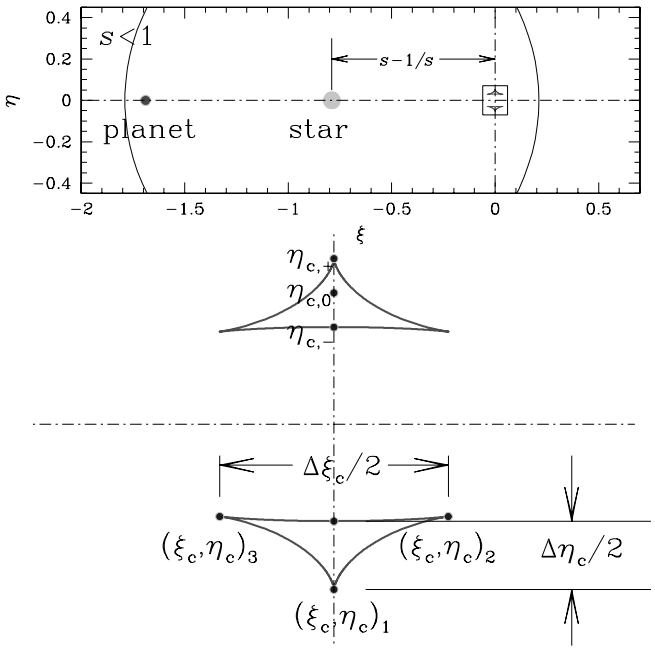

FIG. 2.—Same as Fig. 1, but for the location and shape of the planetary caustic of a planetary system with a star-planet separation less than the Einstein ring radius ($s < 1$). [*See the electronic edition of the Journal for a color version of this figure*.]

when the planet is located in the "lensing zone," which represents the range of the star-planet separation of $0.6 \lesssim s \lesssim 1.6$. The planetary caustic is always bigger than the central caustic.

3. ANALYTIC APPROACH

We start from the formula of Bozza (2000) for the position of the planetary caustics (eqs. [49] and [50] of his paper). Keeping up to the first-order term, the formulae are expressed as

$$\xi_c \simeq q^{1/2}\left(\kappa - \frac{1}{\kappa} + \frac{\kappa}{s^2}\right)\cos\theta, \tag{1}$$

$$\eta_c \simeq q^{1/2}\left(\kappa - \frac{1}{\kappa} - \frac{\kappa}{s^2}\right)\sin\theta, \tag{2}$$

where θ is a variable and

$$\kappa(\theta) = \left(\frac{\cos 2\theta \pm \sqrt{s^4 - \sin^2 2\theta}}{s^2 - 1/s^2}\right)^{1/2}. \tag{3}$$

In these expressions, the coordinates are centered at the position on the star-planet axis with a separation vector from the position of the star of

$$\boldsymbol{r} = \boldsymbol{s}\left(1 - \frac{1}{s^2}\right), \tag{4}$$

where $\boldsymbol{s}$ is the position vector of the planet from the star normalized by $\theta_{\rm E}$ (see Figs. 1 and 2). The origin of the coordinates corresponds to the center of the planetary caustic. For the pair of the planets with separations s and $1/s$, the centers of the caustics are separated from the star by the same distance [because $|\boldsymbol{r}(s)| = |\boldsymbol{r}(1/s)|$] but directed toward opposite directions (because $\mathrm{sign}[\boldsymbol{r}(s)] \neq \mathrm{sign}[\boldsymbol{r}(1/s)]$). Therefore, the center of the caustic is located on the same and opposite sides of the planet with respect to the position of the star for the planets with $s > 1$ and <1, respectively. If one defines the lensing zone as the range of the planetary separation for which the planetary caustic is located within the Einstein ring, the exact range of the lensing zone is

$$\frac{\sqrt{5} - 1}{2} \leq s \leq \frac{\sqrt{5} + 1}{2}. \tag{5}$$

To the first-order approximation, the size of the planetary caustic is proportional to $q^{1/2}$, as shown in equations (1) and (2). We discuss the deviation of the approximation from the exact value in § 4.3.

3.1. *For Planets with $s > 1$*

In this case, between the two values of κ in equation (3) only the one with a plus sign is valid because the other one with a minus sign results in $\kappa^2 < 0$. As a result, there exists only a single set of caustics for planets with $s > 1$, as shown in Figure 1.

The planetary caustic of the planet with $s > 1$ is composed of four cusps, with two of them located on the ξ-axis and the other two located on the η-axis (see Fig. 1). The positions of the individual cusps, $(\xi_c, \eta_c)_i$, correspond to the cases of $\sin\theta = 0$ (for the two cusps on the ξ-axis) and $\cos\theta = 0$ (for the other two cusps on the η-axis). Then the positions of the cusps on the ξ- and η-axes are expressed respectively as

$$(\xi_c,\ \eta_c)_{1,\,2} \simeq \left(\frac{2q^{1/2}}{s\sqrt{s^2 - 1}},\ 0\right), \tag{6}$$

$$(\xi_c,\ \eta_c)_{3,\,4} \simeq \left(0,\ \frac{2q^{1/2}}{s\sqrt{s^2 + 1}}\right). \tag{7}$$

If we define the horizontal and vertical widths of the planetary caustic as the separations between the cusps on the individual axes (see Fig. 1), the widths are expressed respectively as

$$\Delta\xi_c \simeq \frac{4q^{1/2}}{s\sqrt{s^2-1}} \rightarrow \frac{4q^{1/2}}{s^2}\left(1+\frac{1}{2s^2}\right), \quad (8)$$

$$\Delta\eta_c \simeq \frac{4q^{1/2}}{s\sqrt{s^2+1}} \rightarrow \frac{4q^{1/2}}{s^2}\left(1-\frac{1}{2s^2}\right), \quad (9)$$

where the expressions after the arrow are those evaluated to the first nonvanishing order in s in the limiting case of $s \gg 1$. Then the vertical/horizontal width ratio is expressed as

$$R_c = \frac{\Delta\xi_c}{\Delta\eta_c} \simeq \left(\frac{1-1/s^2}{1+1/s^2}\right)^{1/2} \rightarrow 1-\frac{1}{s^2}. \quad (10)$$

In the limiting case of $s \gg 1$, $\Delta\xi \sim \Delta\eta \propto s^{-2}$ and $R_c \sim 1$; i.e., the caustic size decreases as s^{-2}, and the shape becomes less elongated as the star-planet separation increases.

3.2. *For Planets with $s < 1$*

In this case, κ in equation (3) is valid only in the following range of θ:

$$\theta \pm \frac{\pi}{2} < \frac{1}{2}\sin^{-1}s^2. \quad (11)$$

For θ within this range, there are two possible values of κ corresponding to the signs. As a result, there exist two sets of caustics for planets with $s < 1$: one above and the other below the star-planet axis (see Fig. 2).

Each of the caustics for the planet with $s < 1$ is composed of three cusps. One of them is located on the η-axis, but the other two are not located on either of the axes. The caustic meets the η-axis at $\eta_{c,+} = 2q^{1/2}/[s(1+s^2)^{1/2}]$ and $\eta_{c,-} = 2q^{1/2}(1-s^2)^{1/2}/s$ when $\cos\theta = 0$ (see Fig. 2). Among these two positions, the former corresponds to the cusp, and thus the location of the on-axis cusp is

$$(\xi_c, \eta_c)_1 \simeq \left(0, \pm\frac{2q^{1/2}}{s\sqrt{1+s^2}}\right), \quad (12)$$

where the sign $\pm$ is for the cusps located above and below the star-planet axis, respectively.

If we define the vertical width of the caustic as the separation between the two crossing points at $\eta_{c,+}$ and $\eta_{c,-}$, the width is expressed as

$$\frac{\Delta\eta_c}{2} \simeq \frac{2q^{1/2}}{s}\left(\frac{1}{\sqrt{1+s^2}} - \sqrt{1-s^2}\right) \rightarrow q^{1/2}s^3, \quad (13)$$

where the factor $\frac{1}{2}$ is included because there exist two planetary caustics for planets with $s < 1$ and the expression after the arrow is that evaluated to the first nonvanishing order in s in the case of $s \ll 1$. By defining the center of *each* caustic as the midpoint between the two crossing points (see Fig. 2), its position is expressed as

$$\eta_{c,0} \simeq \pm\frac{q^{1/2}}{s}\left(\frac{1}{\sqrt{1+s^2}} + \sqrt{1-s^2}\right) \rightarrow \frac{2q^{1/2}}{s}\left(1-\frac{1}{2}s^2\right). \quad (14)$$

The other two cusps occurs when $d\xi/d\theta = 0$ (or $d\eta/d\theta = 0$). This condition is satisfied when $\cos^2 2\theta = 1 - 3s^4/4$ (or $\sin^2 2\theta = 3s^4/4$). Then, combined with the possible range in equation (11), the values of θ corresponding to the off-axis cusps are found to be

$$\theta_0 = \frac{\pi}{2} \pm \frac{1}{2}\sin^{-1}\left(\frac{\sqrt{3}}{2}s^2\right). \quad (15)$$

With this value combined with equations (1) and (2), the positions of the off-axis cusps are expressed as

$$(\xi_c, \eta_c)_{2,3} \simeq [\pm q^{1/2}(\kappa_0 - 1/\kappa_0 + \kappa_0/s^2)\cos\theta_0, \pm q^{1/2}(\kappa_0 - 1/\kappa_0 - \kappa_0/s^2)\sin\theta_0], \quad (16)$$

where $\kappa_0 = \kappa(\theta_0)$. In the limiting case of $s \ll 1$, equation (16) is approximated as

$$(\xi_c, \eta_c)_{2,3} \rightarrow \left(\pm\frac{3\sqrt{3}q^{1/2}s^3}{8}, \pm\frac{2q^{1/2}}{s}\right), \quad (17)$$

because $\kappa_0 \rightarrow s(1+s^2/4)$, $\sin\theta_0 \rightarrow 1$, and $\cos\theta_0 \rightarrow \sqrt{3}s^2/4$. By defining the horizontal width as the separation between the two off-axis cusps, the width is expressed as

$$\frac{\Delta\xi_c}{2} \simeq 2q^{1/2}\left(\kappa_0 - \frac{1}{\kappa_0} + \frac{\kappa_0}{s^2}\right)\cos\theta_0 \rightarrow \frac{3\sqrt{3}}{4}q^{1/2}s^3. \quad (18)$$

Once again, the factor $\frac{1}{2}$ is included because there are two planetary caustics. From equations (13) and (18), the vertical/horizontal width ratio is expressed as

$$R_c \simeq \frac{(1+s^2)^{-1/2} - (1-s^2)^{1/2}}{s(\kappa_0 - 1/\kappa_0 + \kappa_0/s^2)\cos\theta_0} \rightarrow \frac{4}{3\sqrt{3}}\left(1-\frac{5}{12}s^2\right). \quad (19)$$

In the limiting case of $s \ll 1$, each caustic shrinks as $\propto s^3$, cf. $\propto s^{-2}$ for planets with $s > 1$, and $R_c \sim 4/3\sqrt{3} \sim 0.770$, cf. $R_c \sim 1$ for planets with $s > 1$.

4. CAUSTIC PROPERTIES IN PLANETARY LENSING

Based on the analytic expressions derived in § 3, we now investigate how the properties of the planetary caustics such as the location, size, and shape vary depending on s and q. We also compare the properties of the planetary caustics with those of the central caustics.

4.1. *Properties of Planetary Caustics*

In the top panel of Figure 3, we present example planetary caustics of several planetary systems with different s and q. In the bottom panel, we present the separation of the caustic from the planet-hosting star as a function of s. In Figure 4, we also present the variation of the caustic size (as measured by the horizontal and vertical widths) and the shape (as measured by the vertical/horizontal width ratio) as a function of s.

The properties of the planetary caustics found from the figures and the dependence of these properties on the planet parameters are as follows.

1. For $s > 1$, the location of the caustic center depends on s but not on q. On the other hand, for planets with $s < 1$, the

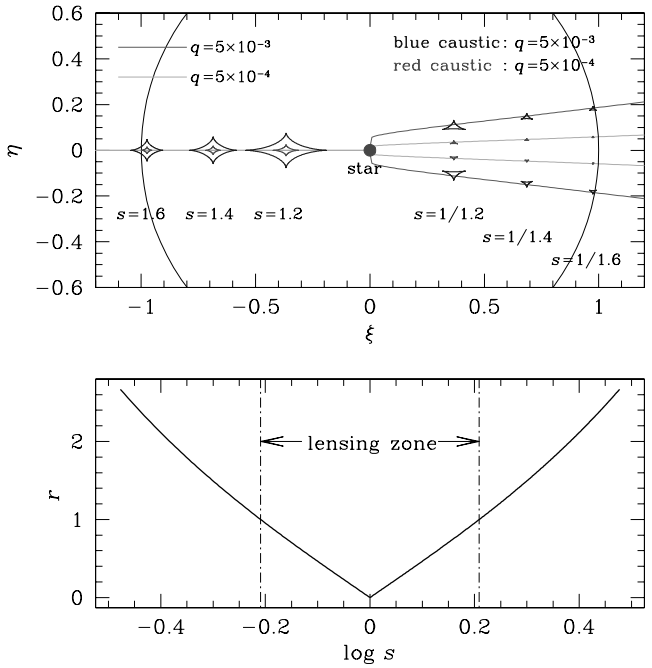

FIG. 3.—*Top*: Example planetary caustics of several planetary systems with different values of the star-planet separation s and the planet/star mass ratio q. The orange and purple curves represent the loci of the center of the caustic as a function of s for planets with $q = 5 \times 10^{-3}$ and 5×10^{-4}, respectively. The coordinates are centered at the position of the planet-hosting star. The circle is the Einstein ring. *Bottom*: Separation between the caustic center and the position of the planet-hosting star as a function of s. [*See the electronic edition of the Journal for a color version of this figure.*]

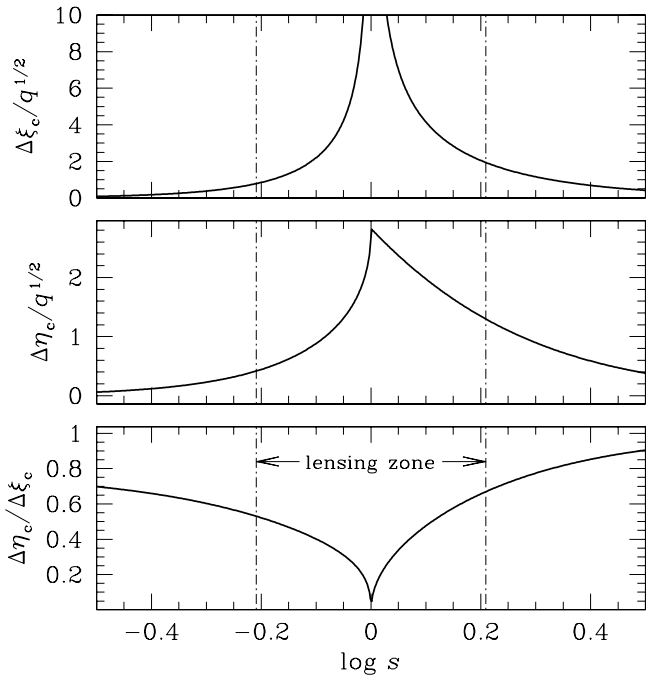

FIG. 4.—Variation of the size (normalized by $q^{1/2}$) and shape (as measured by the vertical/horizontal width ratio) of the planetary caustic as a function of the star-planet separation s.

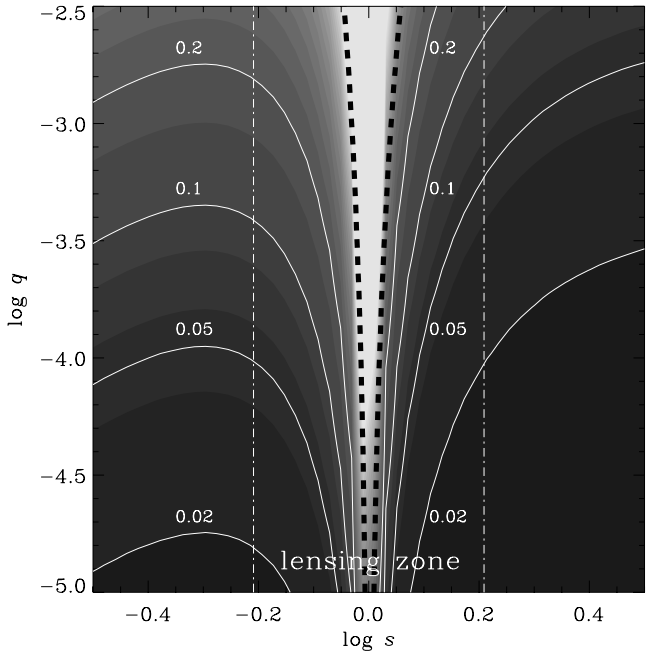

FIG. 5.—Size ratio between the planetary and central caustics as a function of the star-planet separation s and planet/star mass ratio q. For a representative quantity of the caustic size, we use the horizontal width. The region enclosed by the thick dashed lines represents the area in which the planetary and central caustics merge together, resulting in gradual obliteration of the distinction between the two types of caustics.

caustic location depends on both s and q. In this case, the caustic is located farther away from the star-planet axis as q increases (see eq. [14]).

2. Although the caustic size depends on the mass ratio as $\propto q^{1/2}$, the shape of the caustic does not depend on q and is solely dependent on s (see eqs. [10] and [19]).

3. The rate of decrease of the caustic size with the increase of $|\log s|$ is different for planets with $s > 1$ and <1. Compared to the caustic of the planet with $s > 1$, the rate of decrease is steeper for the planet with $s < 1$. In the limiting cases of $s \gg 1$ and $\ll 1$, the caustic sizes decrease as $\propto s^{-2}$ and $\propto s^{3}$, respectively (see eqs. [8], [9], [13], and [18]).

4.2. *Comparison with Central Caustics*

Chung et al. (2005) presented analytic expressions for the location, cusp positions, width, and shape of the central caustics analogous to those presented in § 3 for the planetary caustics. The expressions for the location of the central caustic, analogous to equations (1) and (2) for the planetary caustic, are

$$\xi_c \simeq q \frac{s + 1/s + 2(\cos^3\phi - 2\cos\phi)}{(s + 1/s - 2\cos\phi)^2}, \tag{20}$$

$$\eta_c \simeq -q \frac{2\sin^3\phi}{(s + 1/s - 2\cos\phi)^2}, \tag{21}$$

where ϕ is a variable and the coordinates are centered at the position of the host star. There exists a single central caustic regardless of s, and it has an elongated asteroid shape with four cusps, of which two are located on the ξ-axis and the other two are off the axis. The analytic expressions for the positions of the individual cusps, which are analogous to equations (6) and (7)

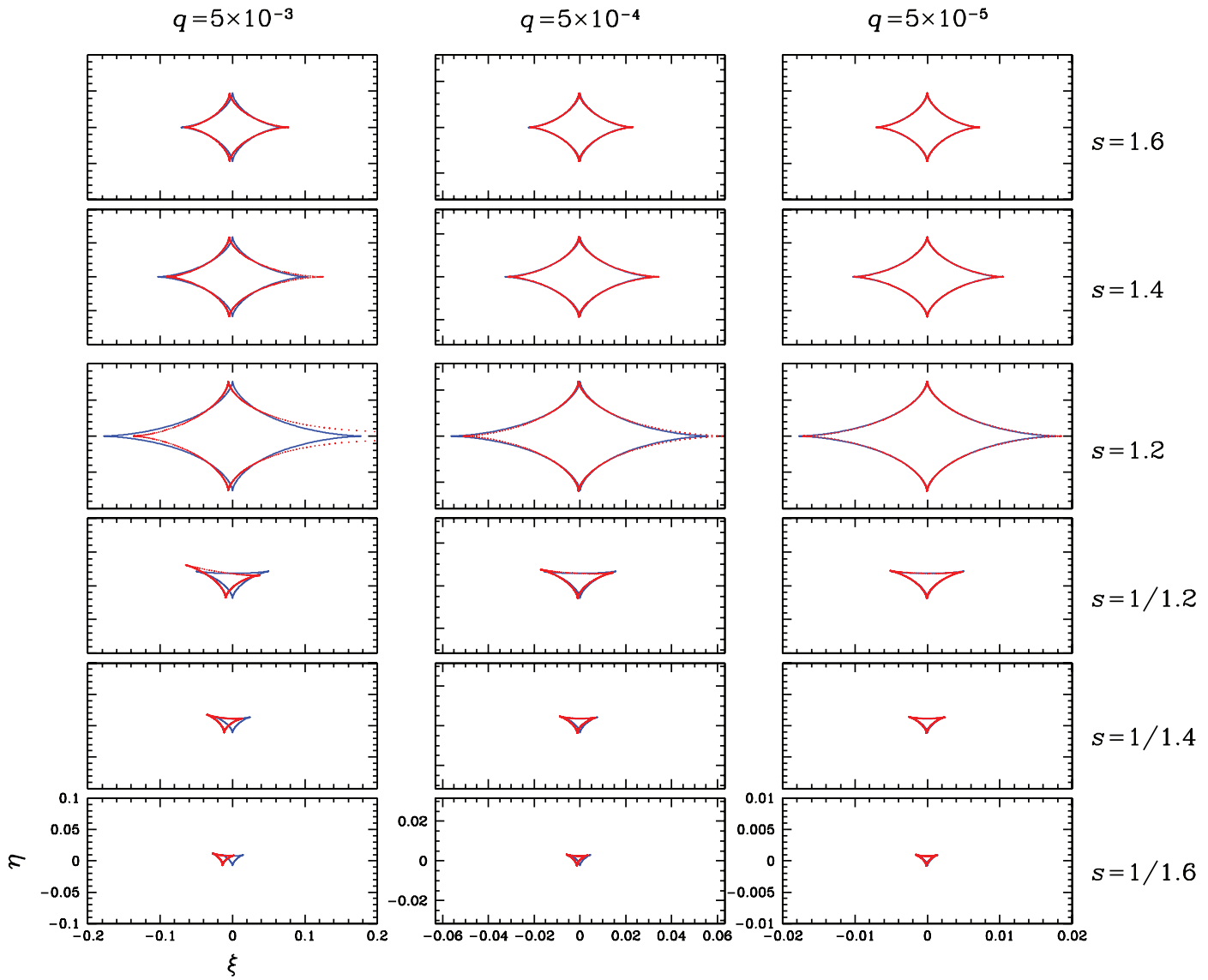

FIG. 6.—Comparison of the planetary caustics based on the analytic (*blue caustic*) and numerical (*red caustic*) computations for various values of the star-planet separation s and the planet/star mass ratio q. The coordinates are centered at the center of the individual caustics. The scales of the individual panels are set so that the caustics with the same s appear to have the same size.

for the planetary caustic with $s > 1$ and to equations (12) and (16) for the planetary caustic with $s < 1$, are

$$(\xi_c,\ \eta_c)_{1,2} \sim \left[\pm\frac{q}{(1\pm s)(1\pm 1/s)},\ 0\right], \tag{22}$$

$$(\xi_c,\ \eta_c)_{3,4} \sim \left[0,\ \pm\frac{2q|\sin^3\phi_c|}{(s+1/s-2\cos\phi_c)^2}\right], \tag{23}$$

where

$$\cos\phi_c = (3/4)(s+1/s)\{1-[1-(32/9)(s+1/s)^{-2}]^{1/2}\}.$$

The horizontal and vertical widths of the central caustic, defined as the separations between the cusps on and off the star-planet axis, are expressed respectively as

$$\Delta\xi_c = \frac{4q}{(s-1/s)^2}, \tag{24}$$

$$\Delta\eta_c = \frac{4q}{(s-1/s)^2}\frac{(s-1/s)^2|\sin^3\phi_c|}{(s+1/s-2\cos\phi_c)^2}, \tag{25}$$

which are analogous to those in equations (8) and (9) for the planetary caustic with $s > 1$ and to equations (13) and (18) for the planetary caustic with $s < 1$.

Then the width ratio of the central caustic is

$$R_c = \frac{(s-1/s)^2|\sin^3\phi_c|}{(s+1/s-2\cos\phi_c)^2}, \tag{26}$$

which is analogous to those in equations (10) and (19) for the planetary caustics with $s > 1$ and $s < 1$, respectively. In the limiting cases of $s \gg 1$ and $\ll 1$, the size of the central caustic decreases as

$$\Delta\xi_c \sim \Delta\eta_c \rightarrow \begin{cases} 4q/s^2 & \text{for } s \gg 1, \\ 4qs^2 & \text{for } s \ll 1. \end{cases} \tag{27}$$

The planetary and central caustics have the following similarities and differences.

1. Unlike the planetary caustic, the pair of the central caustics with separations s and $1/s$ are identical as demonstrated by the

fact that the inversion $s \leftrightarrow 1/s$ in equations (20) and (21) results in the same expressions.

2. While the dependence of the size of the planetary caustic on the planet/star mass ratio is $\propto q^{1/2}$, the dependence of the central caustic is $\propto q$. Therefore, the planetary caustic shrinks much more slowly with the decrease of the planet mass than the central caustic.

3. For planets with $s > 1$, the rate of decrease of the size of the central caustic with the increase of $|\log s|$ is similar to that of the planetary caustic with $s > 1$, i.e., $\Delta\xi \propto s^{-2}$ (see eqs. [8] and [27]), but smaller than that of the planetary caustic with $s < 1$, which shrinks as $\propto s^3$ (see eq. [18]).

Then what is the size ratio between the planetary and central caustics? If we use the horizontal width as a representative quantity for the caustic size, the size ratio between the two types of the caustics is found from equations (8), (18), and (24) and expressed as

$$\frac{\Delta\xi_{c,\,\mathrm{c}}}{\Delta\xi_{c,\,\mathrm{p}}} = \begin{cases} q^{1/2}/(1-s^{-2})^{3/2} & \text{for } s > 1, \\ q^{1/2}/[(s-s^{-1})^2(\kappa_0 - \kappa_0^{-1} + \kappa_0 s^{-2})\cos\theta_0] & \text{for } s < 1, \end{cases} \tag{28}$$

where the additional subscripts p and c denote the planetary and central caustics, respectively. In Figure 5, we present the size ratio as a function of s and q. Since $\Delta\xi_{c,\,\mathrm{c}} \propto q$ while $\Delta\xi_{c,\,\mathrm{p}} \propto q^{1/2}$, the dependence of the size ratio on the mass ratio is $\Delta\xi_{c,\,\mathrm{c}}/\Delta\xi_{c,\,\mathrm{p}} \propto q^{1/2}$. For a given mass ratio, the size ratio is maximized at around $s \sim 1$ and decreases rapidly with the increase of $|\log s|$.[1]

As $s \rightarrow 1$, the location of the planetary caustic, i.e., $\boldsymbol{r} = \boldsymbol{s}(1 - 1/s^2)$, approaches the position of the central star, around which the central caustic is located. Then the two types of the caustics eventually merge together, resulting in gradual loss of distinction between the two types of caustics. The condition for the merging of the two caustics is that the separation between the two caustics is smaller than the half of the sum of the individual caustic widths, i.e.,

$$\frac{\Delta\xi_{c,\,\mathrm{c}} + \Delta\xi_{c,\,\mathrm{p}}}{2} \geq \left| s - \frac{1}{s} \right|. \tag{29}$$

By using the analytic expressions for $\Delta\xi_{c,\,\mathrm{p}}$ (eqs. [8] and [18]) and $\Delta\xi_{c,\,\mathrm{c}}$ (eq. [24]), we compute the region of the caustic merging in the parameter space of (s, q) and present it in Figure 5 (the region enclosed by thick dashed lines). The region is confined in a small region around $|\boldsymbol{s}| \sim 1$, but the width of the region increases as q increases because the caustic size increases with the increase of q.

[1] For the case of $s < 1$, the change rate of the size ratio is reversed as $|\log s|$ further increases beyond a critical value ($|\log s| \sim -0.3$ or $s \sim 0.5$). However, this reversal occurs at the separation beyond the lensing zone.

4.3. *Validity of the Approximation*

Are the presented analytic expressions based on perturbational approximation good enough for the description of the caustics in planetary microlensing? We answer this question by comparing the two sets of caustics constructed based on analytic and numerical computations.

In Figure 6, we present some pairs of the planetary caustics with different values of the planet parameters s and q. In each panel of the figure, the blue caustic is drawn by using the analytic expressions, while the red caustic is the exact one based on numerical computations. For reference, we note that the mass ratios of the planets with masses equivalent to Jupiter, Saturn, Neptune, and Earth around a host star with $\sim 0.3\ M_\odot$ of the most probable Galactic lensing event, are $q \sim 3 \times 10^{-3}$, 10^{-3}, 2×10^{-5}, and 10^{-5}, respectively. From the figure, we find that although the deviation increases with the increase of the planet/star mass ratio, the analytic approximation well describes the planetary caustic in most of the planets' mass regime [$q \lesssim O(10^{-3})$]. For the Earth-mass planet, we find that the two caustics are eventually indistinguishable.

5. CONCLUSION

We derived analytic expressions for the location, size, and shape of the planetary caustic as a function of the star-planet separation and the planet/star mass ratio under perturbational approximation. Based on these expressions, we conducted comprehensive analysis on the properties of the planetary caustics. Combined with the analogous expressions for the central caustics derived in Paper I, we compared the similarities and differences between the planetary and central caustics. We also presented the expressions for the size ratio between the two types of caustics and for the condition of the merging of the two types of caustics. These analytic expressions will be useful in understanding the dependence of the planetary lensing behavior on the planet parameters and thus in interpreting the planetary lensing signals.

We would like to thank J. H. An and A. Gould for making helpful comments. Work by C. H. was supported by the Astrophysical Research Center for the Structure and Evolution of the Cosmos (ARCSEC) of the Korea Science and Engineering Foundation (KOSEF) through the Science Research Center (SRC) program.

REFERENCES

An, J. H. 2005, MNRAS, 356, 1409
Asada, H. 2002, ApJ, 573, 825
Bond, I. A., et al. 2004, ApJ, 606, L155
Bozza, V. 2000, A&A, 355, 423
Chung, S.-J., et al. 2005, ApJ, 630, 535 (Paper I)
Dominik, M. 1999, A&A, 349, 108
Gould, A., & Loeb, A. 1992, ApJ, 396, 104
Mao, S., & Paczyński, B. 1991, ApJ, 374, L37
Udalski, A., et al. 2005, ApJ, 628, L109